



OPEN

Deep learning for pulmonary embolism detection on computed tomography pulmonary angiogram: a systematic review and meta-analysis

Shelly Soffer^{1,2,3✉}, Eyal Klang^{3,4,5,6,7}, Orit Shimon^{5,8}, Yiftach Barash^{3,4,5}, Noa Cahan⁹, Hayit Greenspan⁹ & Eli Konen^{4,5}

Computed tomographic pulmonary angiography (CTPA) is the gold standard for pulmonary embolism (PE) diagnosis. However, this diagnosis is susceptible to misdiagnosis. In this study, we aimed to perform a systematic review of current literature applying deep learning for the diagnosis of PE on CTPA. MEDLINE/PUBMED were searched for studies that reported on the accuracy of deep learning algorithms for PE on CTPA. The risk of bias was evaluated using the QUADAS-2 tool. Pooled sensitivity and specificity were calculated. Summary receiver operating characteristic curves were plotted. Seven studies met our inclusion criteria. A total of 36,847 CTPA studies were analyzed. All studies were retrospective. Five studies provided enough data to calculate summary estimates. The pooled sensitivity and specificity for PE detection were 0.88 (95% CI 0.803–0.927) and 0.86 (95% CI 0.756–0.924), respectively. Most studies had a high risk of bias. Our study suggests that deep learning models can detect PE on CTPA with satisfactory sensitivity and an acceptable number of false positive cases. Yet, these are only preliminary retrospective works, indicating the need for future research to determine the clinical impact of automated PE detection on patient care. Deep learning models are gradually being implemented in hospital systems, and it is important to understand the strengths and limitations of these algorithms.

Pulmonary embolism (PE) is associated with significant morbidity and mortality^{1,2}. Prompt and accurate diagnosis allows for expediting treatment. This is critical as it could substantially reduce mortality and improve outcomes³.

Computed tomographic pulmonary angiography (CTPA) has become the gold standard diagnostic modality for PE^{4–6}. CTPA is a non-invasive, widely available, and rapidly acquired modality. However, the diagnosis of PE in CTPA is time-consuming and requires radiologists' expertise. As a result, the interpretation process is susceptible to errors and delayed diagnosis^{7,8}.

In the past few years, artificial intelligence (AI) has made a significant impact on healthcare. Specifically, deep learning algorithms, which excel at pattern recognition, are revolutionizing medical imaging analysis^{9,10}.

Deep learning technology presents an innovative approach to PE detection. In this review, we present a short description of AI fundamentals followed by a literature review evaluating studies that analyzed deep learning algorithms for PE on CTPA.

¹Internal Medicine B, Assuta Medical Center, Samson Assuta Ashdod University Hospital, Ashdod, Israel. ²Ben-Gurion University of the Negev, Be'er Sheva, Israel. ³Deep Vision Lab, The Chaim Sheba Medical Center, Ramat Gan, Israel. ⁴Department of Diagnostic Imaging, Sheba Medical Center, Tel Hashomer, Israel. ⁵Sackler Medical School, Tel Aviv University, Tel Aviv, Israel. ⁶Department of Population Health Science and Policy, Institute for Healthcare Delivery Science, Mount Sinai, New York, NY, USA. ⁷Sheba Talpiot Medical Leadership Program, Tel Hashomer, Israel. ⁸Department of Anesthesia, Rabin Medical Center, Beilinson Hospital, Petah Tikva, Israel. ⁹Department of Biomedical Engineering, Faculty of Engineering, Tel-Aviv University, Tel Aviv, Israel. ✉email: soffer.shelly@gmail.com

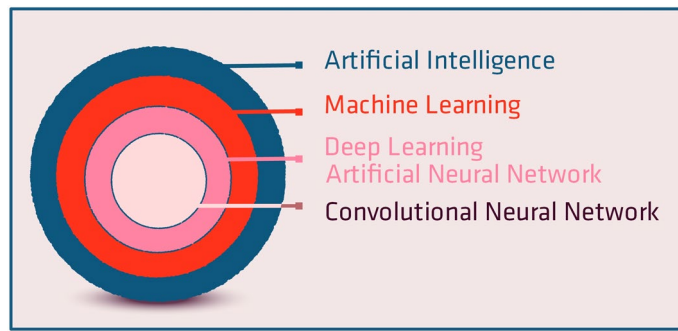


Figure 1. Artificial intelligence (AI) is an umbrella of terms encompassing machine learning and deep learning.

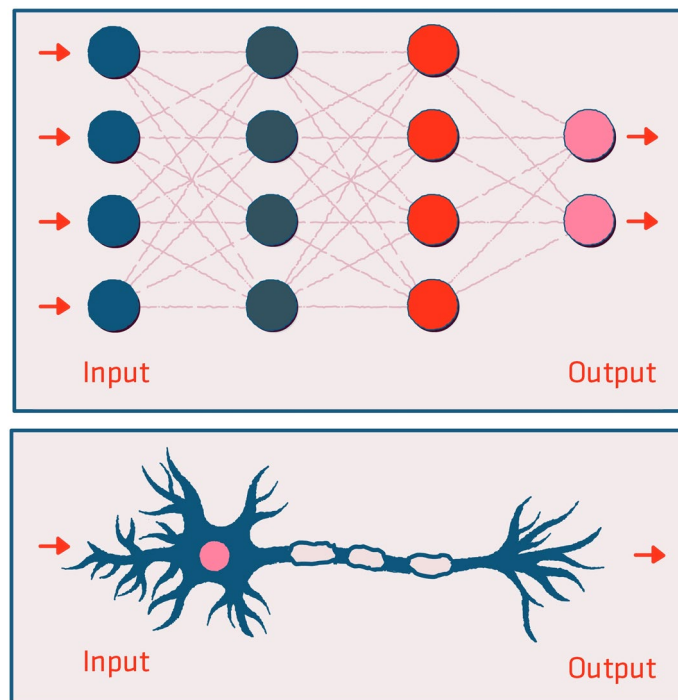


Figure 2. Comparison between artificial and biologic neural networks. Neural networks are comprised of multiple interconnected layers. Data is fed to the network, and an output is produced. By comparing the network's output to the desired true label, an error can be estimated. Based on the error, the algorithm optimizes connections between the layers. The connections between the neurons are termed “weights”. Ultimately, a tuned network is achieved.

Fundamentals of artificial intelligence

Deep learning. AI is a broad term that encompasses a variety of techniques (Fig. 1)¹¹. Deep learning is a subfield of AI which is based on neural networks (Fig. 2). These artificial networks are composed of multiple interconnecting neuron layers. Each neuron is essentially a single linear regression unit. The inputs for each neuron are the outputs of the neurons in the previous layer. The connections between the neurons are termed “weights”.

During training, input data is fed into the network, and the final output is calculated. The difference between the network output (the estimated label) and the true label allows for error estimation. By estimating the error of the model output, the algorithm can optimize the network by tweaking its weights. This process of network optimization is called backpropagation. By tweaking the weights, important network connections are reinforced, while unimportant connections are inhibited. In this way, the difference between the network outputs and the true labels is minimized and the network's error decreases^{12,13}.

Convolutional neural networks. Convolutional neural networks (CNN) are the hallmark deep learning networks for image analysis. This algorithm was invented in the 90' but made a major impact on the world in the 2012 ImageNet challenge¹⁴. That work, termed “AlexNet”, is now the most ever cited scientific paper¹⁵.

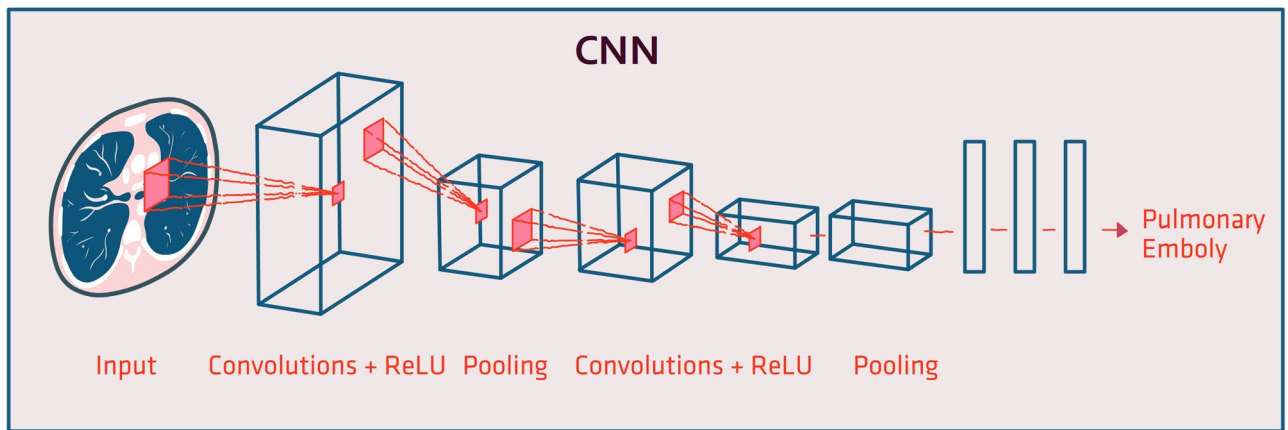


Figure 3. The architecture of Convolutional Neural Network (CNN). CNNs are networks specifically designed to process images. Many small filters compose each CNN layer. A filter is a small matrix of weights that is repeatedly applied to the image pixels. By sharing the filter across the image, repeating patterns are recognized. CNNs are ideal for image analysis since images are composed of repeating patterns. The shallow layers of the CNN recognize low-level patterns. The deeper layers gain a high-level understanding of the image.

CNNs are specifically designed to process images. Each CNN layer contains many filters. Each filter is a small matrix of weights, similar to the general neural networks' weights. The filters are repeatedly applied to image pixels. Since the filters are shared across the image, they recognize repeating patterns. Thus, CNNs are ideal for image analysis, as images are composed of repeating patterns. The shallow layers of the CNN recognize low-level patterns including lines, circles, and other simple geometric patterns. The deeper layers gain a high-level understanding of the image such as context (i.e., “image with PE” vs. “image without PE”) (Fig. 3). In the past few years, CNNs made a dramatic change to medical image analysis¹⁶.

Computer vision. Computer vision is an engineering field dedicated for analyzing images by using computer algorithms such as CNN. Three main computer vision tasks include: classification, detection, and segmentation (Fig. 4)⁹. Classification is the labeling of an entire image. Detection is the localization of an individual object in the image. Segmentation is pixel-wise delineation of the borders of an individual object in the image.

These three tasks can be understood through the analysis of CTPA with PE. The entire scan can be classified as either pathologic (with PE) or normal (no PE). We can further detect individual emboli. Lastly, we can segment the pixel-wise borders of the emboli (Fig. 4).

Methods

This review was conducted according to the Preferred Reporting Items for Systematic Reviews and Meta-Analyses (PRISMA) guidelines¹⁷.

Search strategy. A comprehensive literature search was performed to identify studies evaluating the role of deep learning in detecting PE on CTPE. The search was conducted on February 20, 2021, using the MEDLINE/PubMed databases. Search keywords included “pulmonary embolism” and “deep learning”. Details on complete search strategies are provided in Supplementary Material 1.

Inclusion criteria were studies that (1) evaluated a deep learning model for PE detection on CTPA, (2) were published in English, (3) were peer-reviewed original publications (4) and contained an outcome measure. We excluded non-computer vision articles, non-deep learning articles, and non-original articles. Abstracts were also excluded. Our search was supplemented by a manual search of references of included studies. The study is registered with PROSPERO (CRD42021237369).

Study selection. Two reviewer authors (SS and EK) independently screened the titles and abstracts to determine whether the studies met the inclusion criteria. The full-text article was reviewed when the title met the inclusion criteria or when there was any uncertainty. Disagreements were adjudicated by a third reviewer (YB).

Data extraction. Using a standardized data extraction sheet, the two reviewers (SS and EK) extracted data independently. Data included publication year, study design and location, number of patients, ethical statements, inclusion and exclusion criteria, description of the study population, use of an online database, size of the database, use of an independent test dataset, whether cross-validation was performed, evaluation metrics, and performance results.

Quality assessment and risk of bias. Quality was assessed by the adapted version of the Quality Assessment of Diagnostic Accuracy Studies (QUADAS-2) criteria¹⁸. The studies were also evaluated using the modified Joanna Briggs Institute (JBI) Critical Appraisal checklist for analytical cross-sectional studies^{19,20}.

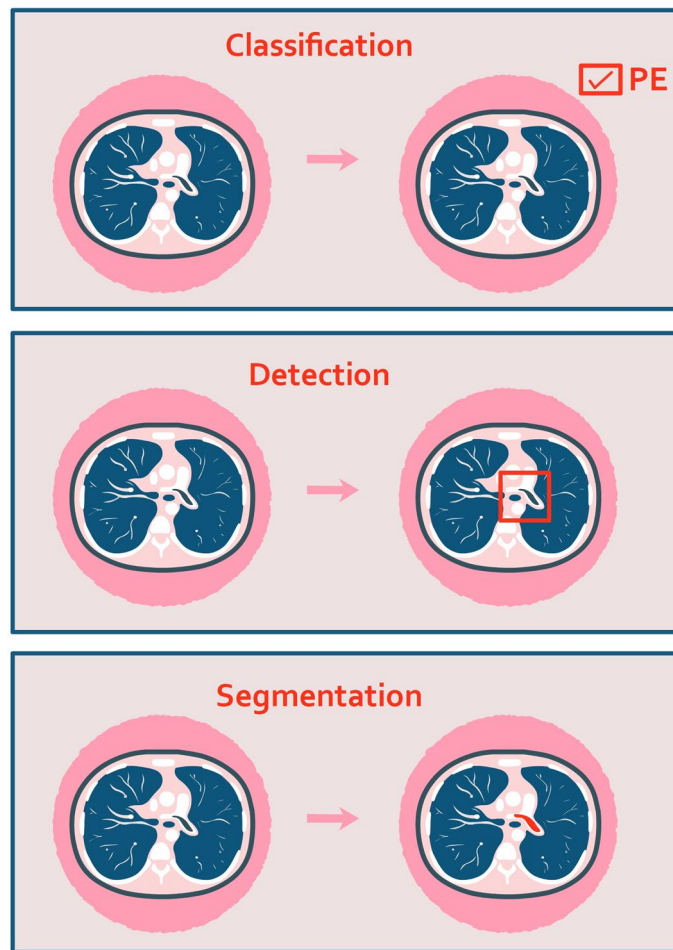


Figure 4. Main computer vision tasks: classification, detection, and segmentation.

Data synthesis and analysis. For the quantitative meta-analysis, we used the R Statistics package *mada*²¹, *meta*, and *metaprop*²². We listed the number of true positive, true negative, false positive, and false negative results per study. Thereafter, we calculated the pooled sensitivity, specificity, and the corresponding 95% CI using the random effect model. A coupled forest plot of sensitivity and specificity was created using RevMan (version 5.3). Summary receiver operating characteristic (ROC) curves were calculated by the bivariate model of Reitsma et al.²³. Heterogeneity was visually checked and evaluated by using I^2 . Values of $I^2 > 50\%$ were considered as significant heterogeneity²⁴.

Results

Study selection and characteristics. The initial literature search resulted in 275 articles. Seven studies met our inclusion criteria (Fig. 5). Studies were published between 2015 and 2020. A total of 36,847 radiographic images were analyzed. Table 1 summarizes the characteristics of the included studies. All the studies were retrospective. In the majority of the studies ($n = 6$, 86%), a board-certified radiologist, served as reference standard.

Descriptive summary of results. Tajbakhsh et al. were the first to apply a CNN solution to detect PE^{25,26}. Using 121 CTPA with 326 individual emboli, they achieved a sensitivity of 83% for detecting individual emboli at two false positives per scan. They have shown that a CNN-based solution outperforms classic machine learning techniques.

Huang et al. utilized a 3D CNN model to detect PE. They used the entire volumetric CTPA imaging data of 1971 patients and achieved an AUROC of 0.85²⁷. Subsequently, they improved their model by integrating imaging data and clinical data from the electronic health record²⁸. The multimodality model showed an AUROC of 0.95, outperforming single modality models.

Liu et al. deployed CNN to detect and calculate the clot burden of PE on CTPA²⁹. Using 878 CTPA with 646 PE, they have shown a sensitivity of 94.6% and a specificity of 76.5%. Additionally, they displayed that the automatic measurement of clot burden was highly correlated with traditional burden scores (Qanadli and Mastora scores).

Weikert et al. developed a CNN algorithm with a relatively large training dataset consisting of 28,000 CTPAs³⁰. They achieved a sensitivity of 92.7% and a specificity of 95.5%. The authors have also performed a sub-analysis

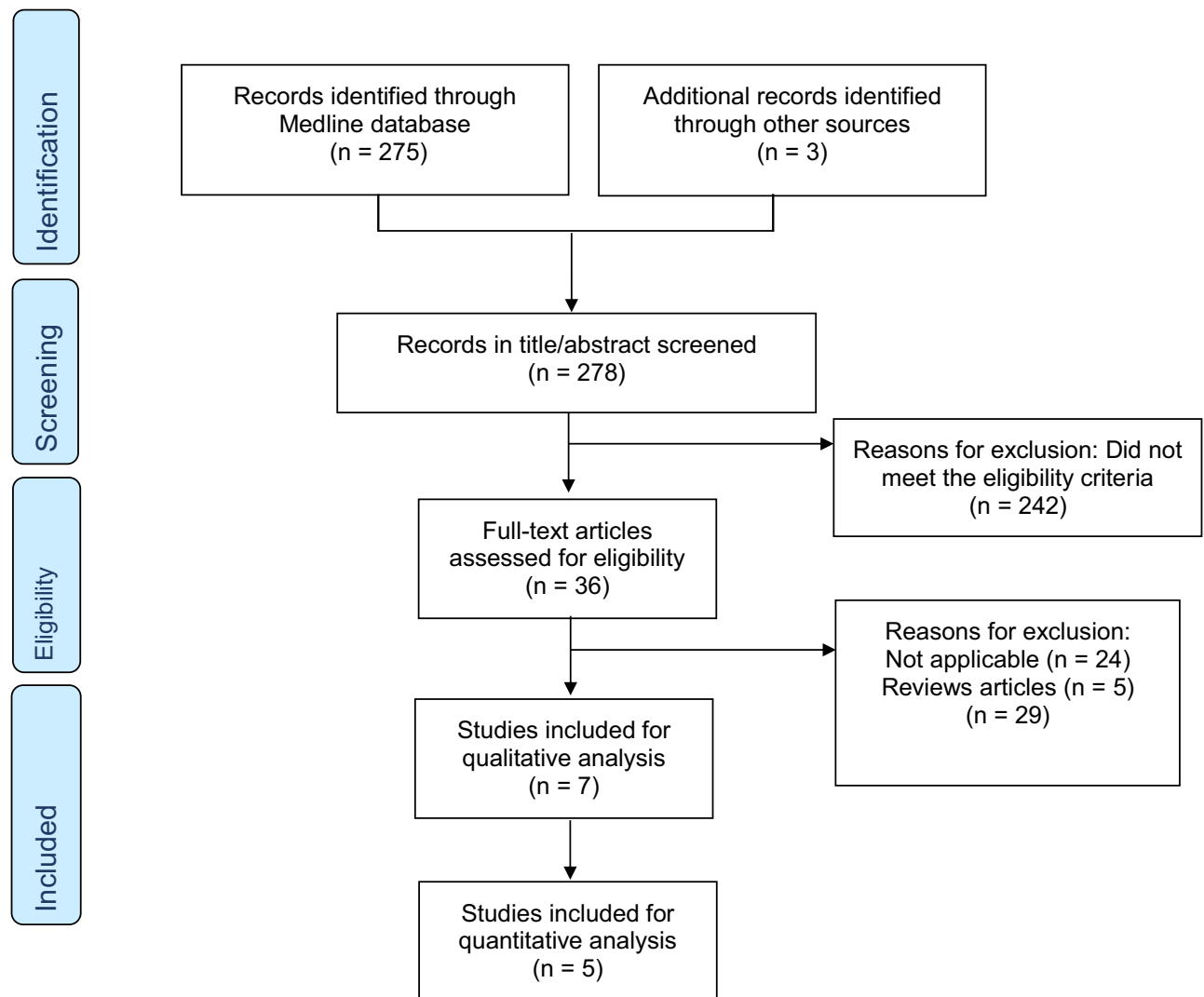


Figure 5. Flow diagram of the search and inclusion process.

| Author | Year | Study design | Database type | Dataset size (n = studies) | Images evaluated by | Performance scores |
|----------------------------------|------|---------------|---------------------------------|----------------------------|--|---|
| Huang et al. ²⁷ | 2020 | Retrospective | Proprietary | 1997 | Board-certified radiologist | AUROC of 0.85 Sensitivity and specificity of 75% and 81% |
| Liu et al. ²⁹ | 2020 | Retrospective | Proprietary | 878 | Delineated by two residents reviewed by an experienced chest radiologist | AUC of 0.93 Sensitivity and specificity of 94.6% and 76.5% |
| Huang et al. ²⁸ | 2020 | Retrospective | Proprietary | 1837 | Board-certified radiologist | AUROC of 0.95 Sensitivity and specificity of 87.3% and 90.2% |
| Weikert et al. ³⁰ | 2019 | Retrospective | Proprietary | 29,465 | Board-certified radiologist | Sensitivity and specificity of 92.7% and 95.5% |
| Yang et al. ⁴⁰ | 2019 | Retrospective | Proprietary + PE challenge data | 129 | Board-certified radiologist | Sensitivity of 75.4% at two false positives per volume |
| Rajan et al. (IBM) ⁴¹ | 2019 | Retrospective | Proprietary | 2420 | Board-certified radiologists | AUC of 0.94 |
| Tajbakhsh et al. ²⁶ | 2019 | Retrospective | Proprietary + PE challenge data | 121 | N/A | Sensitivity of 83% at two false positives per volume |

Table 1. A summary of the articles in the literature review that applied deep learning techniques for pulmonary embolism detection on computed tomographic pulmonary angiography.

A

Forest Plot

| Study | TP | FP | FN | TN | Sensitivity (95% CI) | Specificity (95% CI) | Sensitivity (95% CI) | Specificity (95% CI) |
|-------------------------------|------|-----|-----|------|----------------------|----------------------|----------------------|----------------------|
| Huang et al. [27], 2020 | 96 | 8 | 14 | 72 | 0.87 [0.80, 0.93] | 0.90 [0.81, 0.96] | | |
| Huang et al. [28], 2020 | 71 | 20 | 23 | 86 | 0.76 [0.66, 0.84] | 0.81 [0.72, 0.88] | | |
| Liu et al. [29], 2020 | 176 | 24 | 10 | 78 | 0.95 [0.90, 0.97] | 0.76 [0.67, 0.84] | | |
| Rajan et al. (IBM) [41], 2019 | 1361 | 180 | 314 | 538 | 0.81 [0.79, 0.83] | 0.75 [0.72, 0.78] | | |
| Weikert et al. [30], 2019 | 215 | 55 | 17 | 1178 | 0.93 [0.89, 0.96] | 0.96 [0.94, 0.97] | | |

B

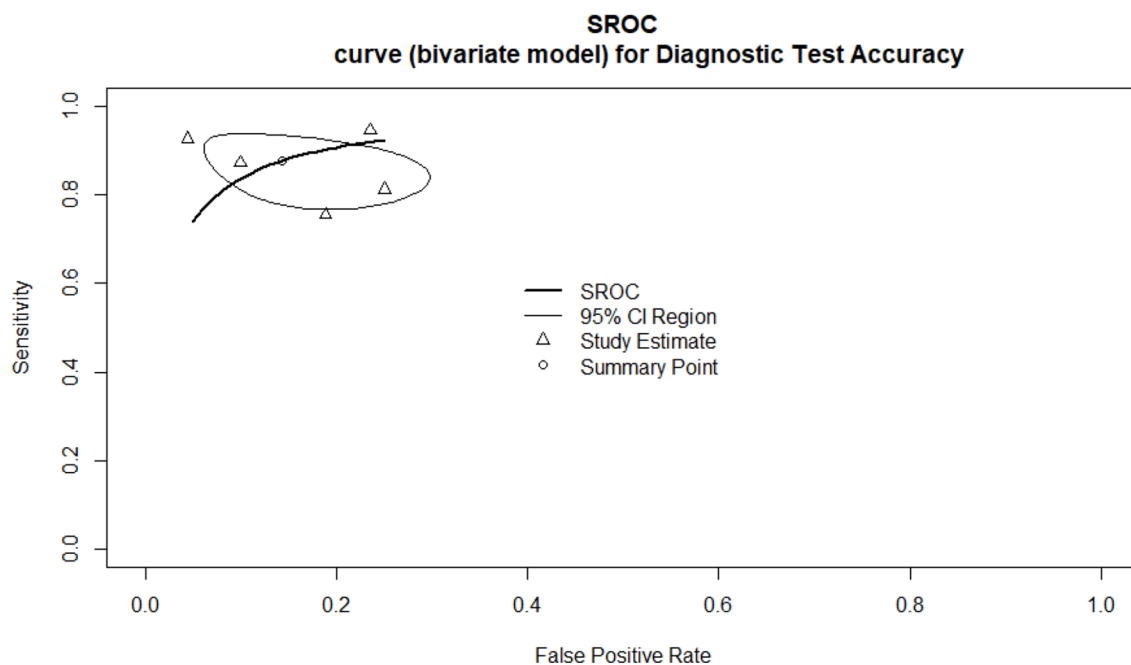


Figure 6. (A) Sensitivity and Specificity of included studies (B) Bivariate summary ROC curves for the detection of pulmonary embolism on CTPA using deep learning.

which revealed that exams containing central emboli had the highest detection rates with 95.7%, followed by segmental emboli with 93.3%. Sub-segmentally located emboli had the lowest detection rate with 85.7%.

Quality assessment. According to the QUADAS-2 tool, five papers scored as high risk of bias in at least one category. Patient selection bias was evident in more than half of the papers, as most studies failed to describe their study population. Most papers also failed in data management as ethical approval was not specified. The objective assessment of the risk of bias is reported in Supplementary Table 1 and Table 2.

Meta-analysis results. Five studies provided enough data to calculate test accuracies. A pooled sensitivity of 0.88 (95% CI 0.803–0.927, $I^2 = 89.6\%$) per scan and a specificity of 0.86 (95% CI 0.756–0.924, $I^2 = 97.4\%$) per scan were shown. Figure 6 presents the sensitivity, specificity, and the bivariate summary ROC curve.

Discussion

Accurate and rapid diagnosis of PE is essential to improve prognosis. Previous research raised the concern that radiologists' interpretation may be impaired by a lack of sensitivity for PE detection. It was demonstrated that the radiologists' sensitivity for detecting PE ranges from 0.67 to 0.87 with a specificity of 0.89 to 0.99^{31–33}. The presented deep learning models provide an automatic approach for identifying PE on CTPA with a pooled sensitivity of 0.88 and specificity of 0.86.

An effective AI system must have an optimal operating threshold that balances between sensitivity and specificity. Such systems can accelerate the diagnostic workflow without burdening the radiologist with false positive cases as a high number of false positives creates alarm fatigue³⁴. For PE detection, it is apparent that a deep learning system can serve as a second reader for the immediate interpretation and prioritization of positive studies. Ultimately, an AI-based tool has the potential to reduce the time to PE diagnosis. Since timely diagnosis is critical, the integration of a triage model can enhance the quality of care. Liu et al. demonstrated that a deep learning model could also flag patients with a worse prognosis according to clot burden or right ventricular dysfunction parameters²⁹.

Early work in automated PE diagnosis was based on traditional machine learning techniques^{35–37}. Commercially available PE detection solutions based on machine learning were also developed^{38–40}. Nonetheless, moderate success with a limited clinical application was achieved. These techniques were tested only on small cohorts. Additionally, even though they achieved clinically acceptable sensitivities, it was at the cost of an extremely high number of false positive cases. Indeed, existing applications were not widely utilized. Deep learning models obtained more promising results with high sensitivity at an acceptable false positive rate.

Although a significant improvement was attained with deep learning, these achievements are limited and are based on a small number of studies. Except for one research²⁸, the studies did not leverage the abundant amount of tabular data on each patient, such as comorbidities and laboratory results. Moreover, all the reviewed studies were retrospective and were not tested in the clinical setting. A direct comparison between the deep learning algorithm and the radiologist performance was not carried out. Multicenter prospective studies are currently missing. It is crucial to evaluate whether an automatic PE detection system can improve the radiologist's performance, ultimately resulting in better clinical outcomes.

In the 2020 annual meeting of the Radiological Society of North America (RSNA), a competition was conducted to detect PE in CTPA studies⁴¹. A large publicly available dataset that included 12,000 CT scans was created for the challenge. These scans were provided by five international medical centers and were annotated by 80 board-certified thoracic radiologists. It is expected that studies based on this public database will be published in the near future.

Several commercial companies also specialize in developing deep learning algorithms to flag and triage urgent PE on CTPA⁴². One company received FDA clearance for their AI tool⁴². In the near future, decision support systems for the detection of PE will be implemented as a second reader. Next, depending on the technology advancement, these systems are expected to replace some of the radiologist's role. For example, in the future, the AI system may have the potential to filter the normal scans with high accuracy, thereby allowing the radiologist to focus on interpreting the abnormal and complicated cases.

Our review has several limitations. All of the reviewed studies were retrospective. The studies' heterogeneity limited assessment of the pooled performance. Half of the studies were at high risk of bias. All studies were conducted in an experimental setting only. Additional studies will be needed to confirm the usefulness of the tool.

In conclusion, deep learning models can detect PE on CTPA with satisfactory sensitivity and an acceptable number of false positive cases. Yet, these are only preliminary retrospective works, indicating the need for future research to determine the clinical impact of automated PE detection on patient care. Deep learning models are gradually being implemented in hospital systems, and it is important to understand the strengths and limitations of these algorithms.

Data availability

All data generated or analysed during this study are included in this published article (and its Supplementary Information files).

Received: 16 April 2021; Accepted: 7 July 2021

Published online: 04 August 2021

References

1. Becattini, C., Vedovati, M. C. & Agnelli, G. Diagnosis and prognosis of acute pulmonary embolism: Focus on serum troponins. *Expert Rev. Mol. Diagn.* **8**, 339–349. <https://doi.org/10.1586/14737159.8.3.339> (2008).
2. Javed, Q. A. & Sista, A. K. Endovascular therapy for acute severe pulmonary embolism. *Int. J. Cardiovasc. Imaging* **35**, 1443–1452 (2019).
3. Agnelli, G. & Becattini, C. Acute pulmonary embolism. *N. Engl. J. Med.* **363**, 266–274. <https://doi.org/10.1056/NEJMra0907731> (2010).
4. Anderson, D. R. *et al.* Computed tomographic pulmonary angiography vs ventilation-perfusion lung scanning in patients with suspected pulmonary embolism: A randomized controlled trial. *JAMA* **298**, 2743–2753 (2007).
5. Schoepf, U. & Costello, P. Spiral computed tomography is the first-line chest imaging test for acute pulmonary embolism: Yes. *J. Thromb. Haemost.* **3**, 7–10 (2005).
6. Schoepf, U. J. Diagnosing pulmonary embolism: Time to rewrite the textbooks. *Int. J. Cardiovasc. Imaging* **21**, 155–163 (2005).
7. Wittram, C. *et al.* CT angiography of pulmonary embolism: Diagnostic criteria and causes of misdiagnosis. *Radiographics* **24**, 1219–1238 (2004).
8. Rufener, S. L., Patel, S., Kazerooni, E. A., Schipper, M. & Kelly, A. M. Comparison of on-call radiology resident and faculty interpretation of 4- and 16-row multidetector CT pulmonary angiography with indirect CT venography. *Acad. Radiol.* **15**, 71–76 (2008).
9. Soffer, S. *et al.* Convolutional neural networks for radiologic images: A radiologist's guide. *Radiology* **290**, 590–606 (2019).
10. Klang, E. Deep learning and medical imaging. *J. Thorac. Dis.* **10**, 1325–1328. <https://doi.org/10.21037/jtd.2018.02.76> (2018).
11. Jordan, M. I. & Mitchell, T. M. Machine learning: Trends, perspectives, and prospects. *Science* **349**, 255–260 (2015).
12. Arel, I., Rose, D. C. & Karnowski, T. P. Deep machine learning—a new frontier in artificial intelligence research. *IEEE Comput. Intell. Mag.* **5**, 13–18 (2010).
13. Hinton, G. E. & Salakhutdinov, R. R. Reducing the dimensionality of data with neural networks. *Science* **313**, 504–507 (2006).
14. Russakovsky, O. *et al.* Imagenet large scale visual recognition challenge. *Int. J. Comput. Vision* **115**, 211–252 (2015).
15. Krizhevsky, A., Sutskever, I. & Hinton, G. E. Imagenet classification with deep convolutional neural networks. *Adv. Neural Inf. Process. Syst.* **25**, 1097–1105 (2012).
16. Ma, J. *et al.* Survey on deep learning for pulmonary medical imaging. *Front. Med.* <https://doi.org/10.1007/s11684-019-0726-4> (2019).
17. Moher, D., Liberati, A., Tetzlaff, J. & Altman, D. G. Preferred reporting items for systematic reviews and meta-analyses: The PRISMA statement. *Ann. Intern. Med.* **151**, 264–269 (2009).
18. Whiting, P. F. *et al.* QUADAS-2: A revised tool for the quality assessment of diagnostic accuracy studies. *Ann. Intern. Med.* **155**, 529–536 (2011).
19. Kwong, M. T., Colopy, G. W., Weber, A. M., Ercole, A. & Bergmann, J. H. The efficacy and effectiveness of machine learning for weaning in mechanically ventilated patients at the intensive care unit: A systematic review. *Bio-Design Manuf.* **2**, 31–40 (2019).

20. Soffer, S. *et al.* Deep learning for wireless capsule endoscopy: A systematic review and meta-analysis. *Gastrointest. Endosc.* **92**(4), 831–839 (2020).
21. Doebler, P. & Holling, H. Meta-analysis of diagnostic accuracy with mada. *R Packag* **1**, 15 (2015).
22. Nyaga, V., Arbyn, M. & Aerts, M. *METAPROP: Stata Module to Perform Fixed and Random Effects Meta-analysis of Proportions* (2017).
23. Reitsma, J. B. *et al.* Bivariate analysis of sensitivity and specificity produces informative summary measures in diagnostic reviews. *J. Clin. Epidemiol.* **58**, 982–990 (2005).
24. Ioannidis, J. P., Patsopoulos, N. A. & Evangelou, E. Uncertainty in heterogeneity estimates in meta-analyses. *BMJ* **335**, 914–916 (2007).
25. Tajbakhsh, N., Gotway, M. B. & Liang, J. Computer-aided pulmonary embolism detection using a novel vessel-aligned multi-planar image representation and convolutional neural networks. In *International Conference on Medical Image Computing and Computer-Assisted Intervention* 62–69 (Springer, 2015).
26. Tajbakhsh, N., Shin, J. Y., Gotway, M. B. & Liang, J. Computer-aided detection and visualization of pulmonary embolism using a novel, compact, and discriminative image representation. *Med. Image Anal.* <https://doi.org/10.1016/j.media.2019.101541> (2019).
27. Huang, S. C. *et al.* PENet—A scalable deep-learning model for automated diagnosis of pulmonary embolism using volumetric CT imaging. *npj Digit. Med.* <https://doi.org/10.1038/s41746-020-0266-y> (2020).
28. Huang, S.-C., Pareek, A., Zamanian, R., Banerjee, I. & Lungren, M. P. Multimodal fusion with deep neural networks for leveraging CT imaging and electronic health record: A case-study in pulmonary embolism detection. *Sci. Rep.* **10**, 1–9 (2020).
29. Liu, W. *et al.* Evaluation of acute pulmonary embolism and clot burden on CTPA with deep learning. *Eur. Radiol.* **30**, 3567–3575. <https://doi.org/10.1007/s00330-020-06699-8> (2020).
30. Weikert, T. *et al.* Automated detection of pulmonary embolism in CT pulmonary angiograms using an AI-powered algorithm. *Eur. Radiol.* **30**, 6545–6553 (2020).
31. Kligerman, S. J. *et al.* Radiologist performance in the detection of pulmonary embolism. *J. Thorac. Imaging* **33**, 350–357 (2018).
32. Das, M. *et al.* Computer-aided detection of pulmonary embolism: Influence on radiologists' detection performance with respect to vessel segments. *Eur. Radiol.* **18**, 1350–1355 (2008).
33. Eng, J. *et al.* Accuracy of CT in the diagnosis of pulmonary embolism: A systematic literature review. *Am. J. Roentgenol.* **183**, 1819–1827 (2004).
34. Mitka, M. Joint commission warns of alarm fatigue: Multitude of alarms from monitoring devices problematic. *JAMA* **309**, 2315–2316 (2013).
35. Özkan, H., Osman, O., Şahin, S. & Boz, A. F. A novel method for pulmonary embolism detection in CTA images. *Comput. Methods Programs Biomed.* **113**, 757–766 (2014).
36. Lahiji, K., Kligerman, S., Jeudy, J. & White, C. Improved accuracy of pulmonary embolism computer-aided detection using iterative reconstruction compared with filtered back projection. *Am. J. Roentgenol.* **203**, 763–771 (2014).
37. Kligerman, S. J., Lahiji, K., Galvin, J. R., Stokum, C. & White, C. S. Missed pulmonary emboli on CT angiography: Assessment with pulmonary embolism-computer-aided detection. *Am. J. Roentgenol.* **202**, 65–73 (2014).
38. Wittenberg, R. *et al.* Acute pulmonary embolism: Effect of a computer-assisted detection prototype on diagnosis—An observer study. *Radiology* **262**, 305–313 (2012).
39. Lee, C. W. *et al.* Evaluation of computer-aided detection and dual energy software in detection of peripheral pulmonary embolism on dual-energy pulmonary CT angiography. *Eur. Radiol.* **21**, 54–62 (2011).
40. Wittenberg, R. *et al.* Stand-alone performance of a computer-assisted detection prototype for detection of acute pulmonary embolism: A multi-institutional comparison. *Br. J. Radiol.* **85**, 758–764 (2012).
41. Colak, E. *et al.* The RSNA pulmonary embolism CT (RSPECT) dataset. *Radiol. Artif. Intell.* e200254 (2021).
42. aidoc. *Pulmonary Embolism Guidelines and the Intersection with AI*, <https://www.aidoc.com/blog/pulmonary-embolism-guidelines-and-the-intersection-with-ai/> (2021).

Author contributions

S.S. had full access to all of the data in the study and takes responsibility for the integrity of the data and the accuracy of the data analysis. Concept and design: S.S., E.Y.K., E.L.K. Acquisition, analysis, or interpretation of data: Y.B., E.Y.K., S.S. Drafting of the manuscript: S.S., E.Y.K., E.L.K. Critical revision of the manuscript for important intellectual content: S.S., Y.B., E.Y.K., E.L.K., O.S., H.G., N.C. Administrative, technical, or material support: S.S., Y.B., E.Y.K., E.L.K., O.S., H.G., N.C. Supervision: E.Y.K.

Competing interests

The authors declare no competing interests.

Additional information

Supplementary Information The online version contains supplementary material available at <https://doi.org/10.1038/s41598-021-95249-3>.

Correspondence and requests for materials should be addressed to S.S.

Reprints and permissions information is available at www.nature.com/reprints.

Publisher's note Springer Nature remains neutral with regard to jurisdictional claims in published maps and institutional affiliations.



Open Access This article is licensed under a Creative Commons Attribution 4.0 International License, which permits use, sharing, adaptation, distribution and reproduction in any medium or format, as long as you give appropriate credit to the original author(s) and the source, provide a link to the Creative Commons licence, and indicate if changes were made. The images or other third party material in this article are included in the article's Creative Commons licence, unless indicated otherwise in a credit line to the material. If material is not included in the article's Creative Commons licence and your intended use is not permitted by statutory regulation or exceeds the permitted use, you will need to obtain permission directly from the copyright holder. To view a copy of this licence, visit <http://creativecommons.org/licenses/by/4.0/>.

© The Author(s) 2021